Technical Note

Thermal Theory for Non-Boussinesq Gravity Currents Propagating on Inclined Boundaries

Albert Dai[1]

Abstract: In this study the author derived the thermal theory for non-Boussinesq gravity currents produced from an instantaneous buoyancy source propagating on an inclined boundary. For Boussinesq gravity currents on a slope, it is known that the gravity current front location history follows an asymptotic relationship, $x_f^{3/2} \sim t$, where x_f is the front location, and t is the time, when the gravity current is sufficiently far into the deceleration phase. For non-Boussinesq gravity currents, the distance for the acceleration phase is extended attributable to the non-Boussinesq effects. When the gravity current is sufficiently far into the deceleration phase, this paper shows that the non-Boussinesq gravity currents tend to approach similar asymptote in the deceleration phase as Boussinesq gravity currents, but the approach is less rapid in non-Boussinesq gravity currents. **DOI: 10.1061/(ASCE)HY.1943-7900.0000949.** *© 2014 American Society of Civil Engineers.*

Author keywords: Thermal theory; Non-Boussinesq gravity currents; Gravity currents; Gravitational convection.

Introduction

Gravity currents, also known as density currents, are buoyancy-driven flows primarily in the horizontal direction (Huppert 2006). Gravity currents manifest in numerous situations, either as a current of heavy fluid running beneath light ambient fluid, or as a current of light fluid above heavy fluid. There are a number of factors which cause variations in the density of fluid, including temperature differentials, dissolved materials, and suspended sediments. Lock-exchange flows, in which gravity currents are produced from an instantaneous, finite buoyancy source and propagate on a horizontal boundary, have drawn much attention in the literature, e.g., Shin et al. (2004), Marino et al. (2005), Cantero et al. (2007), and La Rocca et al. (2008). Gravity currents on a slope have been considered less, but are also commonly encountered, such as powder-snow avalanches (Hopfinger 1983) and spillage of hazardous materials (Fannelop 1994). For more details about the diversity of gravity currents in geophysical environments and engineering applications, the readers are referred to Allen (1985) and Simpson (1997).

Gravity currents down an inclined boundary can be produced with a continuous inflow (Britter and Linden 1980; Garcia 1993, 1994) or with an instantaneous release of a finite volume of heavy fluid (Beghin et al. 1981; Dai et al. 2012; Dai 2013). For Boussinesq gravity currents produced from an instantaneous buoyancy source propagating on an inclined boundary, Beghin et al. (1981) reported that the gravity currents go through an acceleration phase followed by a deceleration phase. Thermal theory for Boussinesq gravity currents, which was developed therein following the famous Morton et al. (1956), has been implemented in related gravity current problems, e.g., Dade et al. (1994) for sediment deposition in gravity currents and Rastello and Hopfinger (2004) for particle-entraining snow avalanches. However, the non-Boussinesq effects were not included in these studies.

More recently, Maxworthy (2010) conducted a series of experiments aiming at Boussinesq gravity currents in the deceleration phase and proposed that the front location history follows a power-relationship. For non-Boussinesq gravity currents, Lowe et al. (2005) and Birman et al. (2005) studied lock-exchange problems on a horizontal boundary with experiments and numerical simulations, respectively. But the geometric configuration makes their problem qualitatively different from that set forth in Beghin et al. (1981) in which thermal theory applies.

Non-Boussinesq gravity currents, in which the density contrasts are relatively larger, are important in quite a few situations. Dense gases are often stored as liquids at low temperatures, and these gases on release could have densities more than twice that of the ambient air. Powder-snow avalanches contain suspended snow grains, and the extra density of the suspended particles is large relative to that of air, even at low concentrations. Volcanic eruptions produce suspended ash and rocks which often take the form of gravity currents. Basically, the Boussinesq approximation does not hold for gravity currents driven by particles in the air when the particle concentration exceeds a few percent (Ancey 2004). Particulate gravity currents can also have considerable destructive potential, e.g., pyroclastic flows and snow avalanches, and understanding the flow dynamics is important for risk assessment in nearby regions (Gladstone et al. 2004). Unlike flows driven by particles in the air, turbidity currents with high sediment concentrations in the water owing to extreme precipitation events may still be considered in the Boussinesq regime (Jacobson and Testik 2013). Previous studies of gravity currents down an inclined boundary have neglected the non-Boussinesq effects. In this study, the author derived the thermal theory for non-Boussinesq gravity currents produced from an instantaneous buoyancy source propagating on an inclined boundary. The influence of non-Boussinesq effects is discussed for the first time with the help of analytical solutions.

Thermal Theory

The configuration of the problem is sketched in Fig. 1. Here the nomenclature primarily follows Beghin et al. (1981) for the reader's convenience. The density of ambient fluid is taken as ρ_0 and the

[1]Associate Professor, Dept. of Engineering Science and Ocean Engineering, National Taiwan Univ., Taipei, Taiwan. E-mail: hdai@mail.tku.edu.tw

Note. This manuscript was submitted on March 20, 2013; approved on August 26, 2014; published online on October 6, 2014. Discussion period open until March 6, 2015; separate discussions must be submitted for individual papers. This technical note is part of the ***Journal of Hydraulic Engineering***, © ASCE, ISSN 0733-9429/06014021(5)/$25.00.

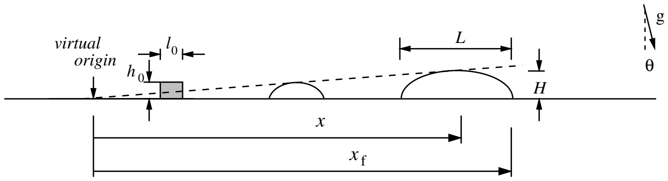

Fig. 1. Sketch of a gravity current produced from a buoyancy source of $A_0 = h_0 l_0$ propagating down a slope which makes an angle θ with the horizontal; the gravity current is assumed to have a semielliptical shape, also known as the *thermal cloud*, with height H and length L; rectangular box represents the initial finite buoyancy

density of heavy fluid in the lock region is ρ_1, where $\epsilon = (\rho_1 - \rho_0)/\rho_0$. The cross-sectional area of the lock, which represents the amount of heavy fluid in the lock, is $A_0 = h_0 l_0$, where h_0 and l_0 are the height and length of the lock, respectively. After an instantaneous removal of the lock gate, the gravity current front develops, and the gravity current head approximately takes a semielliptical shape with a height-to-length aspect ratio, $k = H/L$. Reported values of k range from 0.20 when $\theta = 5°$ to 0.53 when $\theta \approx 90°$, where θ is the slope angle (Beghin et al. 1981). It should be pointed out that the semielliptical shape assumption for the head may not be valid for the non-Boussinesq case with extreme density contrasts. In such a case, the flow patterns may change from a *cloud* to a *wedge* shape (Bonometti et al. 2008), and the mixing between the fluids is very limited.

The convection of gravity current is driven by the heavy fluid contained within the head. Therefore, the linear momentum equation takes the form

$$\frac{d(\rho + k_v \rho_0) S_1 HLU}{dt} = B \sin\theta \tag{1}$$

where ρ = density of mixed fluid in the head; U = mass-center velocity of the head; t = time; $k_v = 2k$ = added mass coefficient (Batchelor 1967); $S_1 = \pi/4$ = shape factor by which the cross-sectional area of the semielliptical head is defined as $S_1 HL$, and $B = g(\rho - \rho_0) S_1 HL$ denotes the buoyancy that is related to the amount of heavy fluid contained in the head. It may be assumed that the amount of heavy fluid in the head is represented by χA_0, i.e., only a fraction χ of heavy fluid in the lock is contained in the head, and the buoyancy is

$$B = \chi g (\rho_1 - \rho_0) A_0 \tag{2}$$

where Beghin et al. (1981) assumed that $\chi = 1$, and Maxworthy (2010) experimentally found that $0.25 \lesssim \chi \lesssim 0.55$ in the deceleration phase. Typically, the parameter χ should be determined by experiments and cannot be evaluated based on theoretical arguments. As such, χ is left unspecified in our framework. Friction on the slope has been considered minor and can be neglected for slope angles greater than a few degrees (Beghin et al. 1981; Ross et al. 2006). With turbulent entrainment assumptions (Ellison and Turner 1959), the mass conservation takes the form

$$\frac{d}{dt}(S_1 HL) = S_2 (HL)^{1/2} \alpha U \tag{3}$$

where $S_2 = (\pi/2^{3/2})(4k^2 + 1)^{1/2}/k^{1/2}$ is another shape factor by which the circumference of semielliptical head is defined as $S_2 (HL)^{1/2}$, and α is the entrainment coefficient.

From Eq. (3)

$$H = \frac{1}{2}\frac{S_2}{S_1} k^{1/2} \alpha x \quad \text{and} \quad L = \frac{1}{2}\frac{S_2}{S_1} k^{-1/2} \alpha x \tag{4}$$

where x = distance from the *virtual origin* to the mass-center of gravity current head. The virtual origin is located x_0 beyond the initial mass-center location of the heavy fluid and can be identified by extrapolating the head height in the upslope direction. Please note that $x_0 \alpha_0 \approx O(h_0)$, where α_0 is the angle of growth. According to Beghin et al. (1981), if the buoyancy could be released with a shape similar to the developed state and with appropriate vorticity, then x_0 would just be the distance from the virtual origin to the position of release. However, this is not possible in practice, and the initial state is situated somewhat downstream of the release gate.

The entrainment coefficient, α, is related to the angle of growth, α_0, through $\alpha_0 = dH/dx$, i.e., $\alpha = [2S_1/S_2 k^{1/2}]\alpha_0$. Upon substitution of Eq. (4) into Eq. (1) and using $U = dx/dt$, the momentum equation becomes

$$U\frac{d}{dx}(x^2 U) + \epsilon\left(\chi \frac{2}{\pi}\frac{k}{1+2k}\frac{A_0}{\alpha_0^2}\right)\frac{dU^2}{dx} = C \tag{5}$$

where

$$C = \frac{4}{\pi}\frac{k}{1+2k}\frac{1}{\alpha_0^2}\chi B_0' \sin\theta \quad \text{with} \quad B_0' = \epsilon g A_0 \tag{6}$$

is the driving force term. It should be pointed out that Eqs. (1) and (5) are consistent with Beghin et al. (1981) and related studies for the Boussinesq case except the second term on the left hand side of Eq. (5), which represents the influence of density difference on the inertia term and has been neglected in previous works.

Boussinesq Case

Eq. (5) may be rearranged in the following form:

$$2xU^2 + \left[\frac{1}{2}x^2 + \epsilon\left(\chi\frac{2}{\pi}\frac{k}{1+2k}\frac{A_0}{\alpha_0^2}\right)\right]\frac{dU^2}{dx} = C \tag{7}$$

after expanding the first term on the left hand side of Eq. (5). When the density difference is sufficiently small such that $\epsilon \ll \pi(1+2k)\alpha_0^2 x^2/4\chi k A_0^2$, the second term on the left hand side of Eq. (7) can be approximated as $0.5x^2 dU^2/dx$, although the right hand side of Eq. (7) remains unchanged. In other words, the influence of the density difference on the inertia term is neglected, although its influence on the driving force term is retained, namely, the Boussinesq case. In this case, the author derived an analytical solution of the form

$$U^2 = U_0^2\left(\frac{x_0}{x}\right)^4 + \frac{2}{3}C\frac{1}{x}\left[1 - \left(\frac{x_0}{x}\right)^3\right] \tag{8}$$

which is identical to the solution given by Beghin et al. (1981) [cf. Eq. (5) therein].

It is worthy to note the condition under which the Boussinesq approximation can be applied, i.e., $\epsilon \ll \pi(1+2k)\alpha_0^2 x^2/4\chi k A_0^2$. Because $x_0\alpha_0 \approx O(h_0)$ and $\pi(1+2k)h_0^2/4\chi k A_0^2 \approx O(1)$, the aforementioned condition for the Boussinesq approximation is equivalent to $\epsilon \ll O(x^2/x_0^2)$. However, a quantitative relationship between ϵ and x_0 is not likely to be built simply based on theoretical arguments without laboratory experiments.

When the buoyancy is released with a quiescent initial condition, i.e., $U_0 = 0$, the gravity current reaches its maximum velocity at $x/x_0 = 4^{1/3}$. In other words, for $1 \le x/x_0 \le 4^{1/3}$, the gravity current is in the acceleration phase, and for $x/x_0 \ge 4^{1/3}$, the gravity current is in the deceleration phase.

For sufficiently large values of x such that $x/x_0 \gg 1$ and with $U_0 = 0$, the solution [Eq. (7)] approaches the following asymptote:

$$U = \frac{\sqrt{2}}{\sqrt{3}}\sqrt{C}x^{-1/2} \tag{9}$$

which can be integrated using $U = dx/dt$ as

$$x^{3/2} = \frac{\sqrt{3}}{\sqrt{2}}\sqrt{C}(t + t_0) \tag{10}$$

where t_0 = integration constant.

Because the front location of the gravity current is a more readily measurable quantity, it is sometimes convenient and desired to write the solution in terms of the front location, x_f. Using the geometric relation $x_f = x + L/2$, the front location, x_f, is related to the mass-center location x through

$$x_f = \left(1 + \frac{\alpha_0}{2k}\right)x \tag{11}$$

If the front location is used rather than the location of the mass-center, Eq. (9) becomes

$$x_f^{3/2} = K_B^{3/2}\chi^{1/2}B_0'^{1/2}(t + t_0) \tag{12}$$

where K_B is expressed in terms of k, α_0, and θ as

$$K_B = \left(\frac{6}{\pi}\right)^{1/3}\left(1 + \frac{\alpha_0}{2k}\right)\left[\frac{k\sin\theta}{(1+2k)\alpha_0^2}\right]^{1/3} \tag{13}$$

Here, it is noted that the relationship between the front location and time [Eq. (12)] is equivalent to the asymptotic form of the velocity in the deceleration phase [Eq. 8)].

Non-Boussinesq Case

Without the Boussinesq approximations, the influence of density variation on the inertia term, $O(\epsilon)$, is retained, and the following closed-form solution is derived:

$$U^2 = U_0^2\left(\frac{1}{2}x_0^2 + \epsilon A_Q\right)^2\left(\frac{1}{2}x^2 + \epsilon A_Q\right)^{-2} + C\left[\frac{1}{6}(x^3 - x_0^3) - \epsilon A_Q(x - x_0)\right]\left(\frac{1}{2}x^2 + \epsilon A_Q\right)^{-2} \tag{14}$$

where U_0 = initial mass-center velocity and $A_Q = 2\chi k A_0/(1+2k)\pi\alpha_0^2$.

When the buoyancy is released with a quiescent initial condition, i.e., $U_0 = 0$

$$\frac{U\sqrt{x_0}}{\sqrt{C}} = \left\{\frac{1}{6}\left(\frac{x}{x_0}\right)^3\left[1 - \left(\frac{x_0}{x}\right)^3\right] + \delta\left(\frac{x}{x_0}\right)\left[1 - \left(\frac{x_0}{x}\right)\right]\right\}^{1/2} \times \left(\frac{x_0}{x}\right)^2\left[\frac{1}{2} + \delta\left(\frac{x_0}{x}\right)^2\right]^{-1} \tag{15}$$

and the location at which a gravity current reaches its maximum velocity, (x_m/x_0), is found through $dU/dx = 0$, i.e.,

$$\left(\frac{x_m}{x_0}\right)^4 + 12\delta\left(\frac{x_m}{x_0}\right)^2 - (4 + 24\delta)\left(\frac{x_m}{x_0}\right) - 12\delta^2 = 0 \tag{16}$$

where $\delta = \epsilon A_Q/x_0^2$, named as effective density difference by the author, is a dimensionless parameter characterizing the non-Boussinesq effects. The Boussinesq case can be interpreted as $\delta \to 0$.

Here, the author gives an estimate for the typical values of δ in different circumstances. Because $x_0\alpha_0 \approx O(h_0)$ and $A_Q/x_0^2 \approx O(1)$, it is estimated that $\delta \approx O(\epsilon)$. Depending on how the gravity currents are produced, the parameter δ assumes a wide range of values in different situations. For example, dense gases are typically stored as liquids with density in the range of 410–500 $\mathrm{kg/m^3}$ at low temperatures, and on release into the atmosphere, these gases could have densities more than twice that of the ambient air, i.e., $\delta \gtrsim 1$. Powder-snow avalanches contain snow grains of which the particle concentration varies between 0.1 and 7%, and the effective density difference varies approximately in the range of $0.5 \lesssim \delta \lesssim 30$. Volcanic eruptions often result in gravity currents with suspended ash and rocks, of which the density of particles ranges approximately from 700 to 3,200 $\mathrm{kg/m^3}$, and the resulting effective density difference is significantly higher, $\delta > 50$. Sediment-laden rivers often form gravity currents in a lake or reservoir, and the sediment concentrations can result in $\delta \lesssim 0.4$. In essence, the effective density difference gives a measure of the non-Boussinesq effects.

Fig. 2 shows (x_m/x_0) versus δ and in the limit as $\delta \to 0$, $(x_m/x_0) \to 4^{1/3}$. It is shown from the thermal theory that the acceleration phase distance is extended for non-Boussinesq gravity currents released with zero momentum.

For sufficiently large values of x such that $x/x_0 \gg 1$, Eq. (14) becomes

$$\frac{U\sqrt{x_0}}{\sqrt{C}} \approx \left[\frac{1}{6}\left(\frac{x}{x_0}\right)^3 + \delta\left(\frac{x}{x_0}\right)\right]^{1/2}\left(\frac{x_0}{x}\right)^2\left[\frac{1}{2} + \delta\left(\frac{x_0}{x}\right)^2\right]^{-1} \tag{17}$$

and when $x^2/x_0^2 \gg 6\delta$, the solution approaches

$$\frac{U\sqrt{x_0}}{\sqrt{C}} \approx \frac{\sqrt{2}}{\sqrt{3}}\left(\frac{x_0}{x}\right)^{1/2} \tag{18}$$

which is the same asymptote as Eq. (8).

It is apparent that for non-Boussinesq gravity currents, the asymptote [Eq. (8)] and consequently Eq. (9) are approached for sufficiently large values of x such that $x/x_0 \gg 1$ and $x^2/x_0^2 \gg 6\delta$. To show the non-Boussinesq effects, Fig. 3 shows $\tilde{U} = Ux_0^{1/2}/C^{1/2}$ versus x/x_0, and Fig. 4 shows $(x/x_0)^{3/2}$ versus $\tilde{t} = tC^{1/2}/x_0^{3/2}$ for $\delta = 0$, 0.5, 1, 2, 3. There is no question that $\tilde{U} \sim (x/x_0)^{-1/2}$, and the relationship in Eq. (12) are approached for sufficiently large values of x. However, it is interesting to

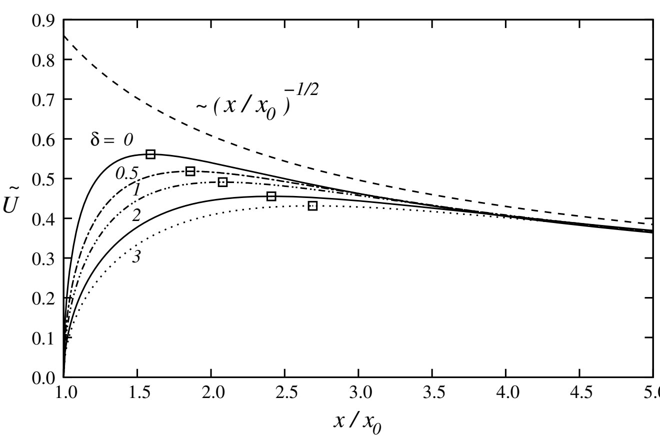

Fig. 2. $(x_m/x_0)^{3/2}$ versus δ; the gravity current reaches its maximum velocity at (x_m/x_0); in the limit as $\delta \to 0$, $(x_m/x_0) \to 4^{1/3}$

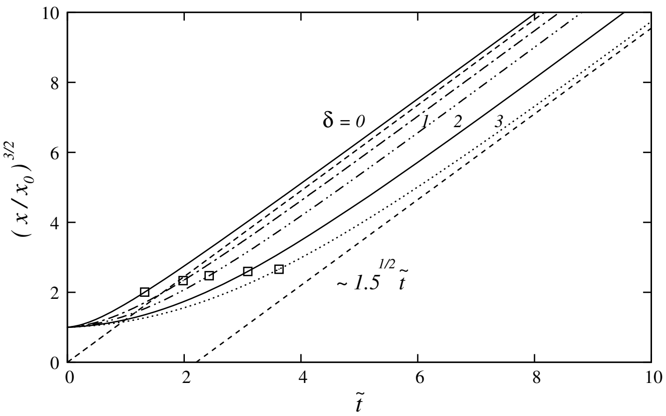

Fig. 3. $\tilde{U} = U x_0^{1/2}/C^{1/2}$ versus x/x_0 for $\delta = 0$, 0.5, 1, 2, 3; symbols: solid line, $\delta = 0$; –.–, $\delta = 0.5$; –..–, $\delta = 1$; – . . . –, $\delta = 2$; . . . , $\delta = 3$; ⊡, location at which the maximum velocity is reached in each case; the dashed line represents the asymptote $\tilde{U} \sim (x/x_0)^{-1/2}$ as the limits $x/x_0 \gg 1$ and $x^2/x_0^2 \gg 6\delta$ are approached

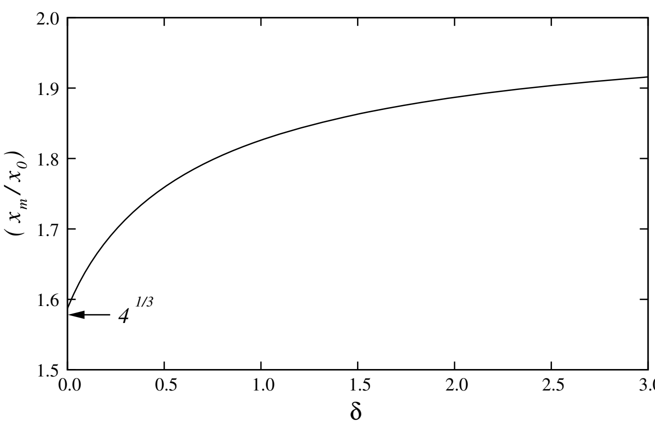

Fig. 4. $(x/x_0)^{3/2}$ versus $\tilde{t} = tC^{1/2}/x_0^{3/2}$ for $\delta = 0$, 0.5, 1, 2, 3; symbols: solid line, $\delta = 0$; –.–, $\delta = 0.5$; –..–, $\delta = 1$; – . . . –, $\delta = 2$; . . . , $\delta = 3$; ⊡, location at which the maximum velocity is reached in each case; the dashed straight lines represent the asymptote $(x/x_0)^{3/2} \sim (\sqrt{3}/\sqrt{2})\tilde{t}$ as the limits $x/x_0 \gg 1$ and $x^2/x_0^2 \gg 6\delta$ are approached

observe that the non-Boussinesq gravity currents tend to approach the asymptotes less rapidly than the Boussinesq gravity currents ($\delta \to 0$). As clearly shown in Fig. 4, the relationship [Eq. (12)] is approached in the deceleration phase more rapidly when $\delta \to 0$ than in other cases when $\delta = 1$, 2, 3.

Summary

In this study the author derived the thermal theory for non-Boussinesq gravity currents produced from an instantaneous buoyancy source propagating on an inclined boundary. For Boussinesq gravity currents propagating on a slope, the front location follows a relationship [Eq. (12)] when the gravity current is sufficiently far into the deceleration phase. For non-Boussinesq gravity currents produced from an instantaneous buoyancy source, the acceleration phase distance is extended. When the gravity current is sufficiently far into the deceleration phase, the author showed that the non-Boussinesq gravity currents approach similar asymptotes in the deceleration phase as Boussinesq gravity currents, but the approach is less rapid.

Acknowledgments

The research is funded in part by the Taiwan Ministry of Science and Technology through grants NSC-101-2628-E-032-003-MY3 and NSC-101-2628-E-002-039-MY3.

References

Allen, J. (1985). *Principles of physical sedimentology*, Allen & Unwin, London.

Ancey, C. (2004). "Powder snow avalanches: Approximation as non-Boussinesq clouds with a richardson number-dependent entrainment function." *J. Geophys. Res.*, 109, F01005.

Batchelor, G. K. (1967). *An introduction to fluid dynamics*, Cambridge University Press, Cambridge, U.K.

Beghin, P., Hopfinger, E. J., and Britter, R. E. (1981). "Gravitational convection from instantaneous sources on inclined boundaries." *J. Fluid Mech.*, 107, 407–422.

Birman, V. K., Martin, J. E., and Meiburg, E. (2005). "The non-Boussinesq lock-exchange problem. Part 2. High-resolution simulations." *J. Fluid Mech.*, 537, 125–144.

Bonometti, T., Balachandar, S., and Magnaudet, J. (2008). "Wall effects in non-Boussinesq density currents." *J. Fluid Mech.*, 616, 445–475.

Britter, R. E., and Linden, P. F. (1980). "The motion of the front of a gravity current travelling down an incline." *J. Fluid Mech.*, 99, 531–543.

Cantero, M., Lee, J., Balachandar, S., and Garcia, M. (2007). "On the front velocity of gravity currents." *J. Fluid Mech.*, 586, 1–39.

Dade, W. B., Lister, J. R., and Huppert, H. E. (1994). "Fine-sediment deposition from gravity surges on uniform slopes." *J. Sediment. Res.*, 64, 423–432.

Dai, A. (2013). "Gravity currents propagating on sloping boundaries." *J. Hydraul. Eng.*, 10.1061/(ASCE)HY.1943-7900.0000716, 593–601.

Dai, A., Ozdemir, C. E., Cantero, M. I., and Balachandar, S. (2012). "Gravity currents from instantaneous sources down a slope." *J. Hydraul. Eng.*, 10.1061/(ASCE)HY.1943-7900.0000500, 237–246.

Ellison, T. H., and Turner, J. S. (1959). "Turbulent entrainment in stratified flows." *J. Fluid Mech.*, 6, 423–448.

Fannelop, T. K. (1994). *Fluid mechanics for industrial safety and environmental protection*, Elsevier, Amsterdam, Netherlands.

Garcia, M. H. (1993). "Hydraulic jumps in sediment-driven bottom currents." *J. Hydraul. Eng.*, 10.1061/(ASCE)0733-9429(1993)119:10(1094), 1094–1117.

Garcia, M. H. (1994). "Depositional turbidity currents laden with poorly sorted sediment." *J. Hydraul. Eng.*, 10.1061/(ASCE)0733-9429(1994)120:11(1240), 1240–1263.

Gladstone, C., Ritchie, L. J., Sparks, R. S. J., and Woods, A. W. (2004). "An experimental investigation of density-stratified inertial gravity currents." *Sedimentology*, 51, 767–789.

Hopfinger, E. J. (1983). "Snow avalanche motion and related phenomena." *Annu. Rev. Fluid Mech.*, 15, 47–76.

Huppert, H. (2006). "Gravity currents: A personal perspective." *J. Fluid Mech.*, 554, 299–322.

Jacobson, M. R., and Testik, F. Y. (2013). "On the concentration structure of high-concentration constant-volume fluid mud gravity currents." *Phys. Fluids*, 25(1), 016602.

La Rocca, M., Adduce, C., Sciortino, G., and Pinzon, A. B. (2008). "Experimental and numerical simulation of three-dimensional gravity currents on smooth and rough bottom." *Phys. Fluids*, 20(10), 106603.

Lowe, R. J., Rottman, J. W., and Linden, P. F. (2005). "The non-Boussinesq lock-exchange problem. Part 1. Theory and experiments." *J. Fluid Mech.*, 537, 101–124.

Marino, B., Thomas, L., and Linden, P. (2005). "The front condition for gravity currents." *J. Fluid Mech.*, 536, 49–78.

Maxworthy, T. (2010). "Experiments on gravity currents propagating down slopes. Part 2. The evolution of a fixed volume of fluid released from closed locks into a long, open channel." *J. Fluid Mech.*, 647, 27–51.

J. Hydraul. Eng., 2015, 141(1): 06014021

Morton, B. R., Taylor, G. I., and Turner, J. S. (1956). "Turbulent gravitational convection from maintained and instantaneous sources." *Proc., R. Soc. A*, 234, 1–23.

Rastello, M., and Hopfinger, E. J. (2004). "Sediment-entraining suspension clouds: A model of powder-snow avalanches." *J. Fluid Mech.*, 509, 181–206.

Ross, A. N., Dalziel, S. B., and Linden, P. F. (2006). "Axisymmetric gravity currents on a cone." *J. Fluid Mech.*, 565, 227–253.

Shin, J., Dalziel, S., and Linden, P. (2004). "Gravity currents produced by lock exchange." *J. Fluid Mech.*, 521, 1–34.

Simpson, J. (1997). *Gravity currents*, 2nd Ed., Cambridge University Press, Cambridge, U.K.